Journal of Thermal Analysis and Calorimetry, Vol. 96 (2009) 2, 427–432

NON-ISOTHERMAL CRYSTALLIZATION OF $K_2O{\cdot}TiO_2{\cdot}3GeO_2$ GLASS

V. D. Živanović[1], S. R. Grujić[2,], M. B. Tošić[1], N. S. Blagojević[2] and J. D. Nikolić[1]*

[1]Institute for the Technology of Nuclear and other Mineral Raw Materials, 86 Franchet d'Esperey, 11000 Belgrade, Serbia
[2]Faculty of Technology and Metallurgy, 4 Karnegijeva St., 11000 Belgrade, Serbia

The crystallization of $K_2O{\cdot}TiO_2{\cdot}3GeO_2$ glass under non-isothermal condition was studied. In powdered glass with particle sizes less than 0.15 mm, surface crystallization was dominant and an activation energy of crystal growth of $E_{a,s}$=327±50 kJ mol^{-1} was calculated. In the size range 0.15 to 0.45 mm, both surface and volume crystallization occurred. For particle sizes >0.45 mm, volume crystallization dominated with spherulitic morphology of the crystals growth and $E_{a,v}$=359±64 kJ mol^{-1} was calculated.

Keywords: *crystallization, glass, kinetics, $K_2TiGe_3O_9$*

Introduction

Previous investigations showed that the ternary germanate glass $K_2O{\cdot}TiO_2{\cdot}3GeO_2$ is very interesting because of its potential application in optoelectronic devices. As reported, $K_2TiGe_3O_9$ nanocrystals are formed on crystallization of this glass [1–3]. The crystallized glass showed second harmonic generations (SHGs), which was induced by the presence of $K_2TiGe_3O_9$ crystals [3]. Accordingly, knowledge of the crystallization process is very important for the preparation of a crystallized glass with the desired microstructure and properties [4]. A study of the nucleation process of this glass showed that homogenous nucleation of $K_2TiGe_3O_9$ crystals occurred with a high steady state nucleation rate I^{max}~10^{15} m^{-3} s^{-1} [5]. Such nucleation behavior is the result of low thermodynamic and kinetic barriers. In the range of high undercooling, crystal growth of $K_2TiGe_3O_9$ with spherical morphology occurred by the mechanism of screw dislocation [6].

This study deals with the crystallization of $K_2O{\cdot}TiO_2{\cdot}3GeO_2$ glass powder under non-isothermal conditions. To clarify in details the crystallization process, differential thermal analysis (DTA), X-ray diffraction (XRD) and scanning electronic microscopy (SEM) methods were employed in the present investigation.

Experimental

The $K_2O{\cdot}TiO_2{\cdot}3GeO_2$ glass was prepared by melting a homogeneous mixture of reagent grade K_2CO_3, TiO_2 (both Fluka Chemicals) and GeO_2 (electronic grade) in a platinum crucible. The melting was performed in an electric furnace BLF 17/3 at T=1300°C during t=2 h. The glass was obtained by quenching the melt on a steel plate. Powder X-ray diffraction (XRD) analysis confirmed the quenched melts to be vitreous. The glass samples were transparent, without visible residual gas bubbles.

The experiments under non-isothermal conditions were performed with a Netzsch STA 409 EP device using Al_2O_3 powder as the reference material. Powdered samples of <0.037, 0.037–0.063, 0.063–0.10, 0.10–0.20, 0.20–0.30, 0.30–0.40, 0.40–0.50, 0.50–0.63, 0.63–0.83, 0.83–1.0 mm were examined. The samples (100 mg) were heated at a heating rate of 10°C min^{-1} from 20 to 800°C. Additionally, the samples of particle sizes of <0.037 and 0.5–0.63 mm were heated at rates of 5, 8, 15 and 20°C min^{-1}.

The XRD method was used to determine the phase composition. The XRD patterns were obtained on a Philips PW-1710 automated diffractometer using a Cu tube operated at 40 kV and 32 mA. The instrument was equipped with a diffracted beam curved graphite monochromator and a Xe-filled proportional counter. The diffraction data were collected in the 2θ Bragg angle range from 4 to 70°, counting for 0.25 s at every 0.02° step. The divergence and receiving slits were fixed at 1 and 0.1 units, respectively. The XRD measurements were performed at room temperature in a stationary sample holder.

A Jeol JSM 6460 microscope was used for the SEM investigations. The fractured bulk samples were used for the SEM analyses. The samples for SEM investigation were gold sputtered.

* Author for correspondence: grujic@tmf.bg.ac.yu

1388–6150/$20.00

Akadémiai Kiadó, Budapest, Hungary
Springer, Dordrecht, The Netherlands

Results and discussion

The results of the chemical analysis show that the composition of the glass was close to stoichiometric for $K_2O{\cdot}TiO_2{\cdot}3GeO_2$, Table 1.

Table 1 Chemical analysis of the glass

	Oxide, x_i/mass%		
	GeO_2	K_2O	TiO_2
Nominal	64.32	19.30	16.37
Analyzed	63.93	19.27	16.80

The XRD analyses of the heat treated glass samples confirmed that $K_2TiGe_3O_9$ crystals were formed [7], Fig. 1. This result indicates that the crystalline phase had the same composition as the parent glass.

Figure 2 shows a SEM microphotograph of a sample thermally treated at T=560°C for time t=110 min, which illustrate the growth morphology in form of a large number of spherically-shaped crystals.

To determine the effect of the particle size on the crystallization mechanism of the powder glass, DTA curves of glass samples of particle sizes 0–1 mm were recorded at a heating rate of v=10°C min^{-1}. All the DTA curves showed only one exothermal peak, appearing in the temperature range T_p=619 - 626°C, Fig. 3.

This curve is similar of the curve obtained for glasses crystallized polymorphically, where T_p increased with increasing particle size, regardless of the dominant crystallization mechanism [8]. Such a behavior can be explained by a decrease in the number of surface nuclei with increasing the particle size and a simultaneous increase in the number of volume nuclei, the total number of nuclei increasing continuously resulting in an increase of the quantitative amount of this phase and its contribution to the DTA signal.

Experimental and theoretical studies have shown that the particle size of powder glass influences the mechanism of its crystallization [9, 10]. In the case of polymorphic crystallization by volume and surface nucleation and interface-limited growth, the height of the exothermal DTA peak $(\delta T)_p$ is proportional to total number of nuclei (volume and surface) contained in the glass particle [10]. Accordingly, the DTA peak height is sensitive to the contributions of these nuclei in the glass particles. The ratio $T_p^2/(\Delta T)_p$, where T_p is the DTA peak temperature and $(\Delta T)_p$ is the half-width of the DTA peak, shows a similar dependency on particle size. This ratio is related to the dimension of crystal growth and can be used as a qualitative measure for surface and volume crystallization [12].

The influence of particle size on the parameters $(\delta T)_p$ and $T_p^2/(\Delta T)_p$ is shown in Fig. 4. From Fig. 4, it can be seen that similar curves, having three regions,

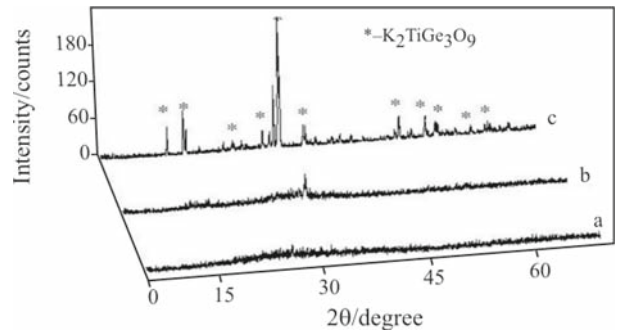

Fig. 1 XRD patterns of: a – the parent glass, b – a sample crystallized at T=560°C for t=110 min and c – a sample crystallized at T=640°C for t=1000 min

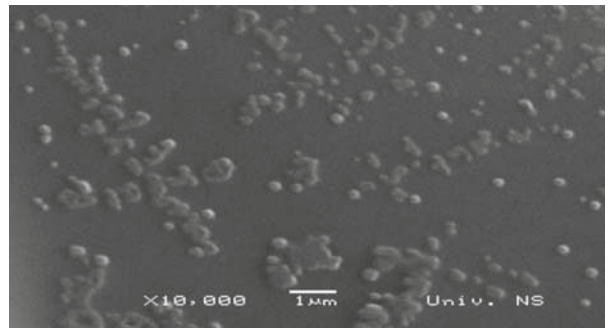

Fig. 2 SEM micrograph of a crystallized glass sample after heat treatment at T=560°C for t=110 min

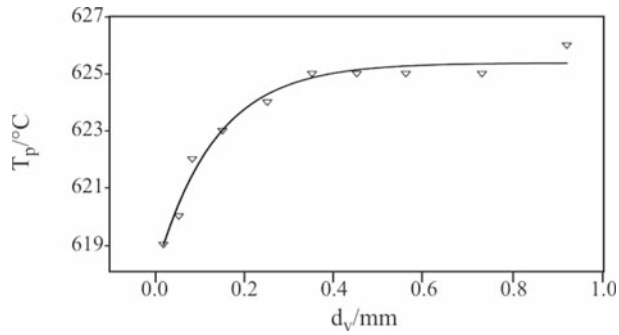

Fig. 3 Effect of particle size on the DTA exothermal peak temperature T_p

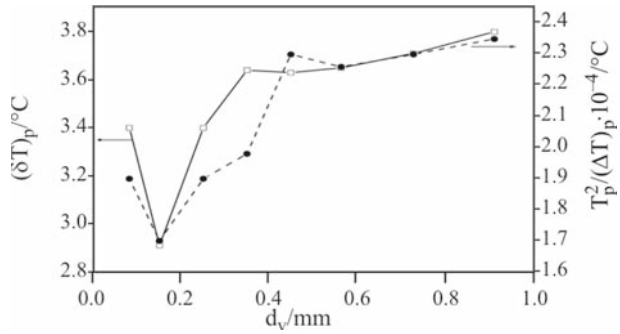

Fig. 4 Effect of particle size on the DTA exothermal peak height $(\delta T)_p$ and the ratio $T_p^2/(\Delta T)_p$

were obtained for both parameters. In the grain size range of 0–0.15 mm (smallest particle sizes, region 1), both parameters decreased with increasing particle size and surface crystallization dominated. Both surface and volume crystallization were important in the size interval 0.15–0.45 mm (region 2), which immediately followed the minimum and extended to the point where the curve nearly attained its asymptotic value. For particle sizes of 0.45–1 mm (region 3), increasing the particle size and volume did not significantly increase the number of volume nuclei or total number of nuclei. Therefore, both parameters $(\delta T)_p$ and $T_p^2/(\Delta T)_p$ remain approximately constant and the volume mechanism of crystallization is dominant.

Based of the results of the effect of particle size on the crystallization mechanism of powder glass, for the determination of the crystallization kinetics under non-isothermal conditions, samples particle sizes of <0.037 mm and 0.5–0.63 mm were chosen. The samples were heated at different heating rates from 20 to 800°C.

The DTA curves of the sample of grain size 0.5–0.63 mm recorded at different heating rates are shown in Fig. 5, from which it may be seen that the crystallization temperature peak, T_p, shifted to higher temperatures with increasing heating rate. A similar behavior was observed for the sample of particle size <0.037 mm. The T_p values recorded at different heating rates for both samples were given in Table 2.

A similar behavior was observed for the sample of particle size <0.037 mm. The T_p values recorded at different heating rates for both samples were given in Table 2.

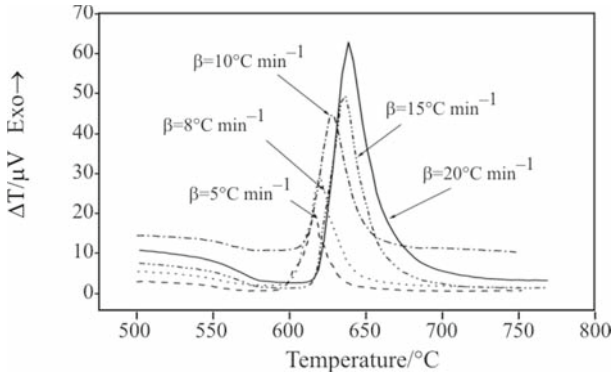

Fig. 5 DTA curves of the powder sample of particle size 0.5–0.63 mm recorded at different heating rates

Table 2 Temperature of the crystallization peak, T_p, for different heating rates β of powder samples of particle size <0.037 and 0.5–0.63 mm

Granulations/ mm		β/°C min^{-1}				
		5	8	10	15	20
<0.037	T_p/°C	616	619	627	637	639
0.5–0.63	T_p/°C	618	623	625	643	647

The majority of the non-isothermal methods has been criticized for assuming an Arrhenian temperature dependence of the transformation kinetics and hence do not have general validity [13, 14]. The temperature dependence of the nucleation rate, I, is far from Arrhenian, and the temperature dependence of the crystal growth rate, U, is also not Arrhenian when a broad range of temperatures is considered. This makes the calculated kinetic parameters reliable and unambiguous only in certain controlled cases. In a sufficiently limited range of temperature (such as the range of crystallization peaks in DTA), both I and U can be described by the approximations:

$$I=I_0\exp(-E_N/RT) \quad (1)$$

and

$$U=U_0\exp(-E_G/RT) \quad (2)$$

where E_N and E_G are the effective activation energies for nucleation and crystal growth, respectively. For the case of isothermal crystallization with I and U independent of time, t, the volume fraction crystallized, x, is given by the Kolmogorov–Johnson–Mehl–Avrami (KJMA) relation:

$$x=1-\exp[-(K_t)^n] \quad (3)$$

where n is the Avrami exponent, which is a dimensionless constant, related to the nucleation and growth mechanisms. Here K is defined as the reaction rate constant, which is usually assigned an Arrhenian temperature dependence [15, 16]:

$$K=K_0\exp(-E/RT) \quad (4)$$

where E is the effective activation energy describing the overall crystallization process. In Eq. (3) $K^n \approx IU^m$, where m denotes the dimensionality of crystal growth. Hence, the assumption of an Arrhenian temperature dependence for K is appropriate when I and U vary in an Arrhenian manner with T. From Eqs (1)–(4), the overall effective activation energy for crystallization is expressed as [17]:

$$E\approx(E_N+mE_G)/n \quad (5)$$

This assumption holds under following of conditions:

- The nucleation rate is negligible, i.e. the condition of site saturation. The occurrence of site saturation in crystal nucleation enables the complicated temperature dependence of the nucleation rate to be neglected and if the temperature dependence of the crystal growth rate is dominated by that of the viscosity, the reaction rate coefficient, K, can reasonably be approximated as Arrhenian over a temperature range around the temperature of the crystallization peak. This condition allows the crystallization process to be considered as an isokinetic reaction, i.e. the crystallization rate is dependent only on

temperature and not on the previous thermal history. The activation energy obtained from DTA method is simply mE_G/n, where E_G is the activation energy of crystal growth.

- When the nucleation rate and the crystal rate have Arrhenian temperature dependences then activation energy, E, is the effective activation energy given by Eq. (5). When the chemical composition of the melt and the crystals are same, the kinetics of crystallization is controlled by interface reactions. For this case, using Eqs (1)–(5) Matusita and Sakka [18, 19], the equation for the analysis of non-isothermal crystallization were derived as:

$$\ln\frac{\beta^n}{T_p^2}=-\frac{mE_a}{RT_p}+\text{const.} \quad (6)$$

where R is the gas constant. The values of parameters n and m depend on the rate controlling mechanism of the crystallization kinetics, while the value of E_a is obtained from the ratio $\ln(\beta^n/T_p^2)$ *vs*. $1/T_p$ using the corresponding values for n and m. In cases when the experiments were performed in such a way that the glass samples were saturated with nuclei before the crystal growth (condition *a*), then parameter E_a may be interpreted as the activation energy of crystal growth.

Accordingly, to satisfy the condition of a constant number of nuclei during crystal growth, the glass powder with smallest particle size of <0.037 mm was chosen. In the range of the smallest granulation, of the total number of nuclei present, the number of surface nuclei is dominant with respect to the internal ones. Therefore, the number of nuclei does not significantly change with heating, while the crystal growth rate becomes considerable. Also, the results of investigations under isothermal conditions indicated that the crystals of $K_2TiGe_3O_9$ are formed by interface-controlled growth. Since, the crystal growth in these DTA experiments occurred on a constant number of nuclei, $n=m=1$ (surface crystallization) and Eq. (6) becomes the same as the well-known Kissinger equation [20]. The T_p temperatures recorded for this sample at different heating rates are presented in Table 2. An activation energy of $K_2TiGe_3O_9$ crystal growth of $E_{a,s}$=327±50 kJ mol^{-1} was calculated by applying the Kissinger equation. Comparing this value of $E_{a,s}$ with the activation energy of $K_2TiGe_3O_9$ crystal growth obtained under isothermal condition, ΔG_D, [5], a difference can be seen. However, the value of $E_{a,s}$ was calculated using a smaller correlation coefficients of 0.97 and a higher standard deviation compared to the calculation of ΔG_D. This indicates that there was a larger scattering of the results in the non-isothermal experiments. Thus, the value of $E_{a,s}$ at the upper scattering limit is in agreement with ΔG_D. Accordingly, it can be concluded that the value of $E_{a,s}$ determined under non-isothermal condition within the range of experimental error is in accordance with the value of ΔG_D, which was determined from isothermal experiments.

For the sample of particle size 0.5–0.63 mm, volume crystallization is dominant i.e., of the total number of nuclei present, the number of volume nuclei is dominant with respect to the surface ones. For this sample, the significant process is volume-homogenous nucleation. A study of the nucleation in this glass [4] showed that volume nucleation occurs in the temperature interval of T=540–610°C. The steady state nucleation rate is very high with a maximum at 582°C. Also, the temperature intervals of nucleation and crystal growth of this glass partly overlap. However, in the temperature interval T=540–582°C, the rate of homogenous nucleation increases, i.e., the number of volume nuclei increases and at 582°C the maximum number of volume nuclei is present in the sample. Above 582°C, the nucleation rate decreases rapidly, so that there is a negligible increase in the number of volume nuclei in the sample. Practically, at T>600°C, the number of volume nuclei in the sample remains constant irrespective of the chosen heating rate. By changing the heating rate, the time for the treatment of the sample in the nucleation temperature range also changes and, consequently, so does the number of volume nuclei in the sample. It was indicated during the DTA experiments that the number of nuclei is inversely proportional to the heating rate. Otherwise, remarkable changes of the growth rate of $K_2TiGe_3O_9$ crystal growth rates occur exactly at temperatures above 582°C. The results of the DTA experiments, Fig. 5 and Table 2, show that the peaks corresponding to crystallization occur at temperatures above 600°C.

For the analysis of the DTA results according Eq. (6), it is necessary to know the values of the parameters n and m. The value of the parameter n may be determined on the basis of the same DTA curves. Parameter n was determined according to the Ozawa method [21] from the following ratio:

$$\left.\frac{\mathrm{d}(\log[-\ln(1-x)])}{\mathrm{d}\log\beta}\right|_T=-n \quad (7)$$

This method avoids the assumption of the temperature dependence of the rate coefficient K. It thus enables a reasonable estimation of parameter n [22]. The volume fraction of crystals, x were obtained from the ratio $x=S/S_0$ where S designates the peak surface at the chosen temperature, while S_0 is the total surface of the corresponding DTA peak. The positions of the crystallization peak on the DTA curves of this sample recorded at heating rates β of 8, 10, 15 and 20°C min^{-1} enabled the determination of four values of x at the selected temperature T=637°C to be determined. The plot

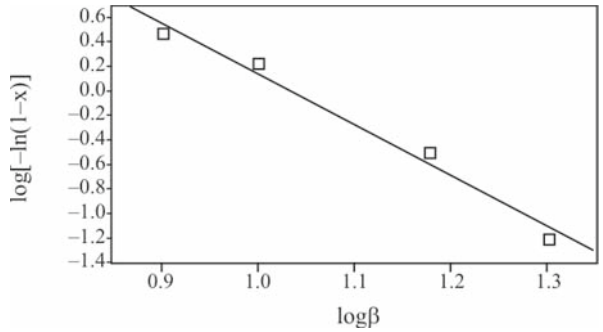

Fig. 6 Plot of log[–ln(1–*x*)] *vs*. logβ at *T*=637°C

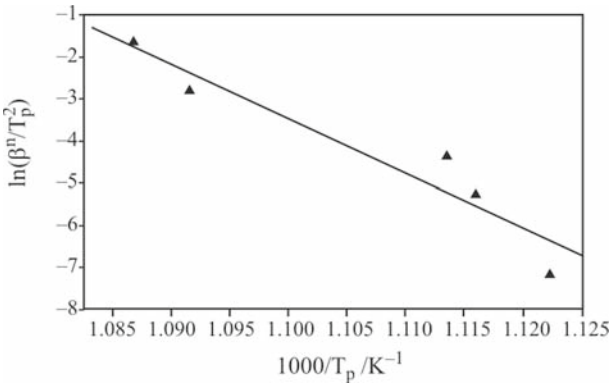

Fig. 7 The plot of $\ln(\beta^4/T_p^2)$ *vs*. $1/T_p$ for a powder sample of particle size 0.5–0.63 mm

Table 3 The activation energy of crystal growth $K_2TiGe_3O_9$ determined for non-isothermal and isothermal conditions

Particle size/mm	DTA activation energy/kJ mol^{-1}		ΔG_D/ kJ mol^{-1}
	Kissinger Eq. (6)	Ozawa Eq. (8)	
<0.037	327±50	–	
0.5–0.63	359±64	379±50	
Bulk [6]	–	–	374±19

of log[–ln(1–*x*)] *vs*. logβ is shown in Fig. 6. From the slope of this plot, the value of *n*=4.15±0.4 was calculated.

Taking into consideration experimental errors, this value is close to *n*=4, which is characteristic for three-dimensional crystal growth controlled by the interface at a nuclei density inversely proportional to the heating rate. For this case *n*=*m*+1. On the basis of the recorded $T_{p,s}$ at various heating rates and the values of parameters *n* and *m*, an activation energy of crystal growth $E_{a,v}$=359±64 kJ mol^{-1} was calculated according to Eq. (6). The plot of $\ln(\beta^4/T_p^2)$ *vs*. $1/T_p$ is shown in Fig. 7.

Also, in this case, the modified Ozawa method [18, 19] can be applied using the relationship:

$$\ln\beta = -(mE_{a,oz}/nRT_p)+\text{const.} \quad (8)$$

Using Eq. (8), the activation energy of crystal growth $E_{a,oz}$=379±50 kJ mol^{-1} was calculated.

The derived values for the activation energy of crystal growth of $K_2TiGe_3O_9$ for isothermal [6] and non-isothermal conditions are summarized in Table 3.

As can be see from Table 3, there is agreement between the activation energy of $K_2TiGe_3O_9$, crystal growth determined under isothermal and non-isothermal conditions, taking into account experimental errors. The activation energy of crystal growth was calculated to be $E_{a,v}$=359±64 kJ mol^{-1}.

Conclusions

Experiments under non-isothermal conditions were performed with powder samples of particle sizes 0–1 mm. The results showed that the particle size of the powder glass influences the mechanism of its crystallization. Three different regions of particle sizes were appeared. For the particle size range of 0–0.15 mm, surface crystallization was dominant. If the particle size are 0.15–0.45 mm, both surface and volume crystallization were significant, while with particle size >0.45 mm, volume crystallization was dominant.

The kinetics of crystallization was examined by DTA under non-isothermal conditions with two powder samples of particle sizes <0.037 mm and 0.5–0.63 mm at different heating rates. The surface crystallization for the sample with particle sizes <0.037 mm and volume one for sizes 0.5–0.6 mm were detected. For both samples the crystallization peaks T_p increased with increasing heating rate. For the sample of particle sizes <0.037 mm, the crystal growth occurred on a constant number of nuclei and the activation energy of crystal growth was calculated as $E_{a,s}$=327±50 kJ mol^{-1}. For the sample particle sizes 0.5–0.63 mm, three-dimensional crystals growth controlled by the interface took place with the nuclei density being inversely proportional to the heating rate and the activation energy of crystal growth was calculated to be $E_{a,v}$=359±64 kJ mol^{-1}. These results show the agreement between the activation energies of $K_2TiGe_3O_9$ crystal growth determined under isothermal and non-isothermal conditions.

Acknowledgements

The authors are grateful to the Ministry of Science, Republic of the Serbia for financial support (Project 142041).

References

1 S. Grujić, N. Blagojević, M. Tošić and V. Živanović, Ceram. Silik., 49 (2005) 270.
2 S. Grujić, N. Blagojević, M. Tošić, V. Živanović and B. Božović, J. Therm. Anal. Cal., 83 (2006) 463.
3 T. Fukushima, Y. Benino, T. Fujiwara, V. Dimitrov and T. Komatsu, J. Solid State Chem. 179 (2006) 3949.
4 L. Stoch and P.Stoch, J. Therm. Anal. Cal., 88 (2007) 577.
5 S. R. Grujić, Ph.D. Thesis, Belgrade University, 2007.
6 S. R.Grujić, N. S. Blagojević, M. B. Tošić, V. D. Živanović and J. D. Nikolić, 39th International October Conference on Mining and Metallurgy-IOCMM 2007, October 07–10, 2007, Sokobanja, Serbia Proceedings, p. 241.
7 JCPDS 27-0394.
8 K. F. Kelton, K. Lakshmi Narayan, L. E. Levin, T. C. Cull and C. S. Ray, J. Non-Cryst. Solids, 204 (1996) 13.
9 C. S. Ray, D. E. Day, W. Haung, K. Lakshmi Narayan, T. C. Cull and K. F. Kelton, J. Non-Cryst. Solids, 204 (1996) 1.
10 C. S. Ray, Q. Yang, W. Haung and D. E. Day, J. Am. Ceram. Soc., 79 (1996) 3155.
11 A. Maroti, A. Buri and F. Branda, J. Mater. Sci., 16 (1981) 341.
12 J. A. Augis and J. E. Bennett, J. Thermal Anal., 13 (1978) 283.
13 M. C. Weiberg, J. Non-Cryst. Solids, 127 (1991) 151.
14 K. F. Kelton, J. Non-Cryst. Solids, 163 (1993) 283.
15 N. Mehta and A. Kumar, J. Therm. Anal. Cal., 83 (2006) 401.
16 N. Mehta and A. Kumar, J. Therm. Anal. Cal., 87 (2007) 343.
17 J. Šesták, Phys. Chem. Glass, 15 (1974) 137.
18 K. Matusita and S. Sakka, Phys. Chem. Glass, 20 (1979) 81.
19 K. Matusita and S. Sakka, J. Non-Cryst. Solids, 34 (1980) 741.
20 H. E. Kissinger, Anal. Chem., 29 (1959) 1072.
21 T. Ozawa, Bull. Chem. Soc. Jpn., 35 (1956) 1881.
22 K. F. Kelton, Mater. Sci. Eng. A, 226–228 (1997) 142.

Received: June 15, 2008
Accepted: September 16, 2008
Online First: January 12, 2009

DOI: 10.1007/s10973-008-9335-1